HIGH-THROUGHPUT AND LABEL-FREE PARASITEMIA QUANTIFICATION AND STAGE DETERMINATION FOR PLASMODIUM FALCIPARUM-INFECTED RED BLOOD CELLS

Xiaonan Yang[1,2], Zhuofa Chen[1], Gihoon Choi[1], Jun Miao[4], Liwang Cui[4] and Weihua Guan[1,3]
[1]The Department of Electrical Engineering, Pennsylvania State University, University Park, USA
[2]School of Information Engineering, Zhengzhou University, Zhengzhou, China.
[3]The Department of Biomedical Engineering, Pennsylvania State University, University Park, USA
[4]The Department of Entomology, Pennsylvania State University, University Park, USA

ABSTRACT

This work reports a high throughput and label-free cell deformability microfluidic sensor for quantitative parasitemia measurement and stage determination for *Plasmodium falciparum*-infected red blood cells (*Pf*-iRBCs). As a mechanical biomarker, the RBC deformability is highly relevant to the infection status. The cell deformability is measured by evaluating the translocation time when each individual cell squeezes through a microscale constriction. More than 30,000 RBCs can be analyzed for parasitemia quantification in under 1 min with a throughput ~500 cells/s. Moreover, the device can also differentiate various malaria stages (ring, trophozoite, and schizont stage) due to their varied deformability. As compared to the microscopy and flow cytometry, this microfluidic deformability sensor would allow for label-free and rapid malaria parasitemia quantification and stage determination at a low-cost.

INTRODUCTION

Malaria is one of the most prevalent infectious diseases for which almost half of the global population is at risk. According to the world malaria report [1], more than 214 million people suffer from malaria infections, and over 400 thousand people died from this preventable disease each year. Parasitemia is a critical parameter for quantifying the parasite load in the organism and indicates the degree of an active parasitic infection. Quantitative measurement of parasitemia and stage determination is important in many phases of malaria assessment, such as the diagnosis and the therapy follow-up, particularly in the chronic phase [2].

The microscopy based morphology analysis still remains the gold standard for parasitemia quantification. Although this approach can identify parasitemia as low as 0.001% [3], it has several drawbacks, including the reliance of an expert reading Giemsa-stained blood smears, subjectivity, low reproducibility and relatively low speed (5 mins/slide) [4]. The flow cytometry was developed to overcome the speed limitation of the microscopy. However, the high cost of the instrumentation and the labeling process limits its widespread usage [5].

It is well known that *Pf*-iRBCs become increasingly rigid (less deformable) as they mature [6], thus the deformability has the potential to be used as a mechanical biomarker to distinguish the healthy and the infected RBCs at various stages. To date, various microfluidic-based methods have been developed to interrogate the cell deformability. For example, non-physical constraint-based interrogation (hydrodynamic pressure, *e.g.*, inertial microfluidics [7], and real-time deformability cytometry [8]), and physical constraint-based interrogation (e.g., single micropore [9], single microchannel [10, 11], and arrayed microchannels [12-14]). Despite success in the qualitative measurement of *Pf*-iRBCs deformability properties, a high throughput quantitative parasitemia measurement has yet to be developed.

In this work, we demonstrated a label-free microfluidic cell deformability sensor for quantitative and high-throughput parasitemia measurement and stage determination for *Pf*-iRBCs. The microfluidic sensor is capable of analyzing more than 30,000 RBCs within 1 mins (throughput ~ 500 cells/s). Moreover, the device is able to differentiate various malaria stages among ring, trophozoite, and schizont stage.

MATERIALS AND METHODS

P. falciparum culture and sample preparation

The *P. falciparum* 3D7 clone was cultured in type O+ human red blood cells in RPMI 1640 medium supplemented with 25 mM HEPES, 50 mg/L hypoxanthine, 25 mM $NaHCO_3$, and 10% (v/v) heat-inactivated type A human serum. The parasite culture was synchronized by treatment of ring-stage parasites with 5% D-sorbitol. The parasites were taken at 2 h, 18 h, and 32 h post synchronization to represent the ring, trophozoites, and schizonts as determined by microscopy. The cultured *P. falciparum* sample prior to electrical sensing measurement consisted of a mixture of *Pf*-iRBCs and uninfected RBCs at a parasitemia of ~12%. The working solution for measurement was 1× phosphate buffer saline (PBS).

Microfluidic device fabrication

The cell deformability sensor was designed in a layout editor and printed on a transparent mask. The polydimethylsiloxane (PDMS) replica was cast out from the SU8 mold. The casting mold was fabricated by a standard double layer lithography process on a 4-inch silicon wafer. SU8 photoresist with a thickness of 5 μm and 25 μm were used for the micropore area and loading channel area, respectively.

The Au/Cr electrodes (20 nm adhesive Cr layer and 80 nm Au layer) were evaporated on a cover glass (thickness ~ 130 μm, Ted Pella) through a laser machined Polymethylmethacrylate (PMMA) shadow mask. To enhance the signal-to-noise ratio, the microelectrodes were positioned close to the micropore area. The PDMS replica was permanently bonded to the cover glass through oxygen plasma treatment.

Electrical measurement and data analysis

A constant voltage (~600 mV DC) was applied across the micropore constriction. The ionic current was monitored as each single individual RBC translocating through the micropore. The ionic current traces were recorded by an amplifier (Axopatch 200B, Molecular Devices, USA). The analog output of the amplifier was sampled with 16-bit DAQ card (NI PCI-6363, National Instruments, USA) and a data acquisition software (LabVIEW) (Figure 1a). The sampling rate for the measurement was 100 kHz. A custom-built MATLAB (MathWorks) program was developed to analyze the data off-line. The translocation time (dwell time) was extracted from each individual cell when translocating the micropore. The time threshold to differentiate the hRBC and the *Pf*-iRBCs was set by the mean value plus three times sigma of the hRBC dwell time (a Gaussian distribution).

RESULTS AND DISCUSSION

Sensing principle

Figure 1 shows the schematic and the corresponding equivalent circuit model for the microfluidic deformability sensor. The device consists of a well-engineered micropore constriction (5×5 μm^2) for the cell to squeeze through. The loading channel's cross-sectional area (1000×25 μm^2) is much larger than that of the micropore to reduce the hydrodynamic and the electrical resistance. The electrical resistance of the microfluidic sensor is mainly dominated by the micropore constriction (*i.e.*, R_{gap} is much larger than other resistances in Figure 1b).

When an RBC squeeze through the micropore, an ionic current dip occur due to the reduced conduction cross-section. In addition, since the micropore has a slightly smaller size than that of the RBCs, the cell translocation time across the micropore is a function of the applied pressure, the cell size and deformability, the pore size, and the PDMS and cell surface properties [15]. Since parameters other than the cell deformability remain almost constant for a given experimental setup, the translocation time is thus an indirect indicator for the cell deformability, *i.e.*, the rigid *Pf*-iRBCs will spend more time (on average) squeezing through the micro-constriction than the more deformable healthy RBCs (hRBCs).

Device characterization

A mixture of polystyrene microbeads with diameters of 5 μm and 10 μm (with a concentration of 1×10^5/ml and 3×10^4/ml, respectively) were used to validate the microfluidic device and the testing apparatus (Figure 1). Figure 2a shows the current trace for the mixed microbeads. Figure 2b shows the scatter plot and the histogram of the dwell time versus current dip amplitude (ΔI). Two separate population can be clearly observed, representing the two different sized microbeads. The percentage of each polystyrene beads measured from the device was consistent with the pre-mixed ratio. This confirmed the functionality of the microfluidic device and the testing apparatus.

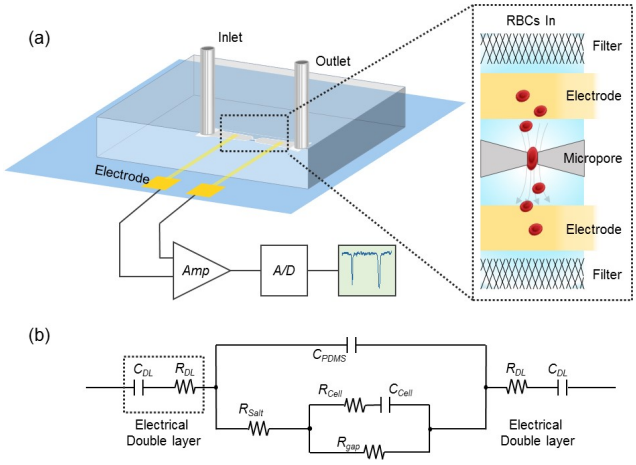

Figure 1. (a) Schematic of the microfluidic cell deformability sensor for highly-throughput and label-free parasitemia quantification. (b) The equivalent circuit model for the sensor.

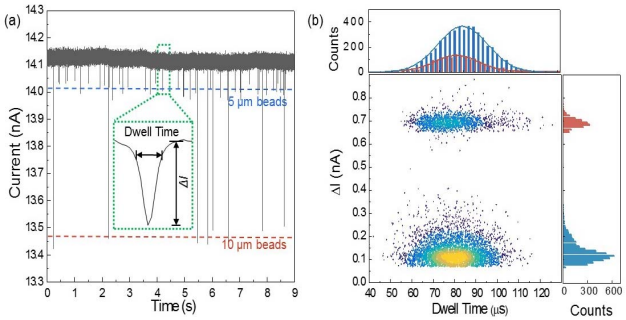

Figure 2. (a) Current traces measured with the mixed microbeads of 5 μm and 10 μm in diameters. (b) The scattering plot and the corresponding histogram for the measurement.

Differentiate ring stage *Pf*-iRBCs and hRBCs

To validate the microfluidic sensor for differentiating ring stage *Pf*-iRBCs and hRBCs, the ring stage *Pf*-iRBCs at 12% parasitemia and the control pure hRBCs were tested. The pressure applied to the device was ~1 psi, leading to a measurement throughput ~500 cells /s in our devices. Figure 3a shows a typical current trace, where the translocation time and the current dip for each single cell can be extracted.

Figure 3b shows the scattering plot of the dwell time and current dip for the pure RBCs (100% hRBCs), while Figure 3c shows the case for the sample at 12% parasitemia (i.e., ~12% *Pf*-iRBCs and ~88% hRBCs). A clear two populations were shown in Figure 3c, representing the *Pf*-iRBCs and hRBCs in samples at 12% parasitemia.

Figure 3d and Figure 3e shows the histogram of the dwell time for the control pure hRBC sample and *Pf*-iRBC sample at 12% parasitemia. The dwell time for the control pure hRBC sample shows a Gaussian distribution with a mean value of 78 μs (Figure 3d). The *Pf*-iRBC sample at 12% parasitemia shows clear two peaks on the dwell time distribution, with mean values of 78 μs and 155 μs, respectively (Figure 3e). These two peaks correspond to the hRBCs and *Pf*-iRBCs, respectively. This result was consistent with the fact that the ring stage *Pf*-iRBCs are less deformable than hRBCs.

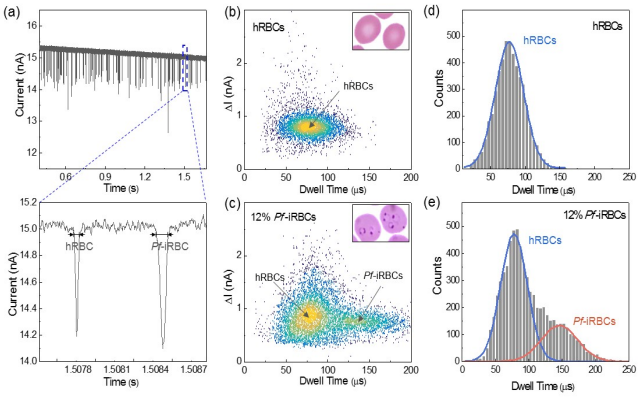

Figure 3. (a) The current trace for Pf-iRBC sample at 12% parasitemia. (b)-(c) The scattering plot of dwell time and current dip for the pure RBC sample (b) and the Pf-iRBC sample at 12% parasitemia (c). (d-e) Histogram plot of dwell time for the pure RBC sample (d) and the Pf-iRBC sample at 12% parasitemia (e).

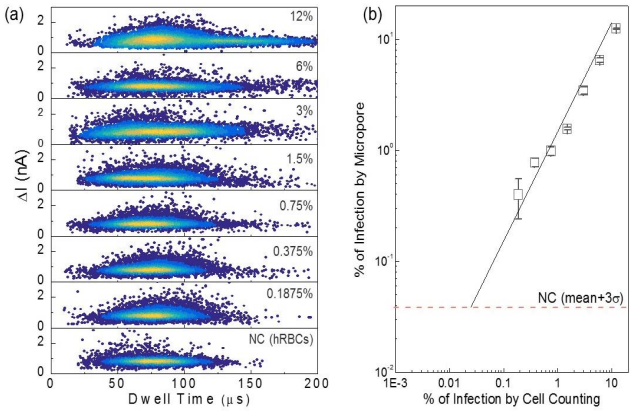

Figure 4. (a) Scattering plot of dwell time versus ΔI for RBCs with parasitemia of 12%, of 6%, 3%, 1.5%, 0.75%, 0.375%, 0.1875% and the healthy RBCs. (b) Parasitemia determined by the microfluidic deformability sensor *versus the parasitemia determined by the microscopy.*

Parasitemia quantification

The microfluidic cell deformability sensor can not only qualitatively differentiate ring stage *Pf*-iRBCs and hRBCs, but also quantitatively determine the parasitemia. With 2× serial dilution of the *Pf*-iRBCs sample at 12% parasitemia, parasitemias of 12%, of 6%, 3%, 1.5%, 0.75%, 0.375%, and 0.1875% were prepared. These samples were tested with the microfluidic cell deformability sensor and translocation time for each parasitemia sample exhibited a similar two-peaked normal distribution. As shown in Figure 4a, a decreasing population with larger translocation time was clearly observed when the sample parasitemia was reduced. The percentage of *Pf*-iRBC population in each sample were obtained by counting the cells of translocation time below a certain threshold. The threshold was determined by the mean value plus three times sigma of the control sample with pure hRBC (a Gaussian distribution). The parasitemia determined by this method was benchmarked with that determined by the microscopy (Figure 4b). The agreement between these two methods demonstrates the microfluidic cell deformability sensor can be used for parasitemia quantification. More than 30,000 RBCs can be analyzed within 1 min. As a comparison, the microfluidic cell deformability sensor is much faster than the microscopy with speed ~ 5 mins/slide [4].

Ability for malaria stage differentiation

In the intraerythrocytic cycle, the *P. falciparum* parasites evolve from ring stage to the trophozoite and finally to the schizont stage. During this process, the stiffness of the red blood cells increases monotonically from 8 μN/m to 16 μN/m at ring stage and finally to 53 μN/m at schizont stage [6]. Therefore, the dwell time of the *Pf*-iRBCs is expected to increase as parasites develop into late stages. We performed the translocation time analysis for the *Pf*-iRBCs at different stages using the microfluidic sensors. Figure 5 shows the dwell time for three different samples, (1) the healthy RBCs (Figure5a-b), (2) the mixture of healthy and ring-stage-only *Pf*-iRBCs (Figure 5c-d), and (3) the mixture of healthy and ring, trophozoite, and schizont stage *Pf*-iRBCs (Figure 5e-f). A clear right-shift of the dwell time can be observed from Figure 5a to Figure 5e. Sub-populations of *Pf*-iRBCs at different stages were clearly distinguishable by multi-peak Gaussian fitting of the dwell time distribution. This observation is consistent with the fact that *Pf*-iRBCs become stiffer as parasites develop into late stages. As a result, the red blood cell deformability could be used as a potential mechanical biomarker to differentiate malaria at different stages.

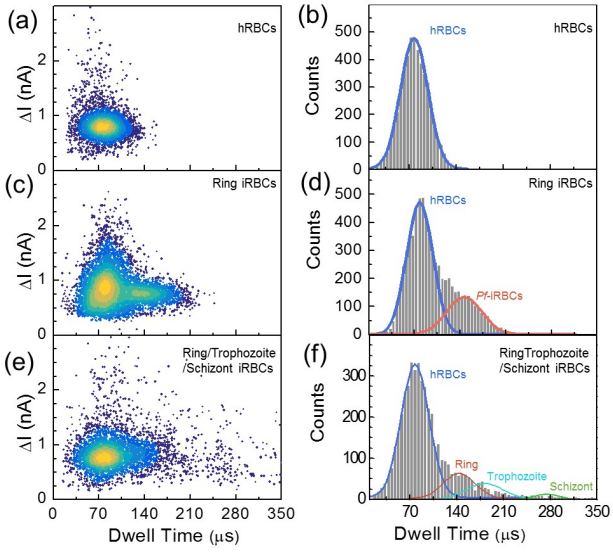

Figure 5. Scattering plot of the current dip versus the translocation time and the corresponding histograms for (a) healthy RBCs, (b) 12% infected ring stage iRBCs, and (c) a mixture of the ring, trophozoite, and schizont stage parasites in RBCs.

CONCLUSION

This work demonstrated an electrofluidic sensor for accurate and quantitative parasitemia measurement. This microfluidic device uses the deformability as the

mechanical biomarker to differentiate the healthy RBCs and *P. falciparum*-infected RBCs. The electrofluidic sensor was able to quantify the parasitemia in a very short amount of time (<1 min) by analyzing a large population of red blood cells (>30 k) in a high throughput (~ 500 cells/s) manner. Moreover, the electrofluidic sensor is able to differentiate various malaria stages. As compared to the microscopy and flow cytometry, this microfluidic device would allow for label-free, rapid and low-cost malaria parasitemia quantification and stage determination.

ACKNOWLEDGEMENTS

This work was partly supported by the Penn State CTSI Grant (UL Tr000127) from the National Center for Advancing Translational Sciences, National Institutes of Health. The content is solely the responsibility of the authors and does not necessarily represent the official views of the NIH. This work is also supported by China Scholarship Council (CSC) and the National Natural Science Foundation of China (Grant No. 61306106).

REFERENCES

[1] World Health Organization. Malaria fact sheet. (2015) Available at: http://www.who.int/malaria/publications/world-malaria-report-2015/en/.

[2] A. E. Bianco, F. L. Battye, and G. V. Brown, "Plasmodium-Falciparum - Rapid Quantification of Parasitemia in Fixed Malaria Cultures by Flow-Cytometry," *Experimental Parasitology,* vol. 62, pp. 275-282, Oct 1986.

[3] W. K. Peng, T. F. Kong, C. S. Ng, L. Chen, Y. Huang, A. A. Bhagat, *et al.*, "Micromagnetic resonance relaxometry for rapid label-free malaria diagnosis," *Nature Medicine,* vol. 20, pp. 1069-+, Sep 2014

[4] W. R. Prescott, R. G. Jordan, M. P. Grobusch, V. M. Chinchilli, I. Kleinschmidt, J. Borovsky*, et al.*, "Performance of a malaria microscopy image analysis slide reading device," *Malar J,* vol. 11, p. 155, May 06 2012.

[5] A. K. Bei, T. M. DeSimone, A. S. Badiane, A. D. Ahouidi, T. Dieye, D. Ndiaye*, et al.*, "A flow cytometry-based assay for measuring invasion of red blood cells by Plasmodium falciparum," *American Journal of Hematology,* vol. 85, pp. 234-237, Apr 2010.

[6] H. W. Hou, A. A. S. Bhagat, A. G. L. Chong, P. Mao, K. S. W. Tan, J. Y. Han*, et al.*, "Deformability based cell margination-A simple microfluidic design for malaria-infected erythrocyte separation," *Lab on a Chip,* vol. 10, pp. 2605-2613, 2010.

[7] D. R. Gossett, H. T. K. Tse, S. A. Lee, Y. Ying, A. G. Lindgren, O. O. Yang*, et al.*, "Hydrodynamic stretching of single cells for large population mechanical phenotyping," *Proceedings of the National Academy of Sciences of the United States of America,* vol. 109, pp. 7630-7635, May 15 2012.

[8] O. Otto, P. Rosendahl, A. Mietke, S. Golfier, C. Herold, D. Klaue*, et al.*, "Real-time deformability cytometry: on-the-fly cell mechanical phenotyping," *Nature Methods,* vol. 12, pp. 199-+, Mar 2015.

[9] V. Faustino, D. Pinho, T. Yaginuma, R. C. Calhelha, I. C. F. R. Ferreira, and R. Lima, "Extensional flow-based microfluidic device: deformability assessment of red blood cells in contact with tumor cells," *Biochip Journal,* vol. 8, pp. 42-47, Mar 20 2014.

[10] Y. Zheng, E. Shojaei-Baghini, A. Azad, C. Wang, and Y. Sun, "High-throughput biophysical measurement of human red blood cells," *Lab on a Chip,* vol. 12, pp. 2560-2567, 2012.

[11] E. Du, S. Ha, M. Diez-Silva, M. Dao, S. Suresh, and A. P. Chandrakasan, "Electric impedance microflow cytometry for characterization of cell disease states," *Lab on a Chip,* vol. 13, pp. 3903-3909, 2013.

[12] Q. Guo, S. J. Reiling, P. Rohrbach, and H. S. Ma, "Microfluidic biomechanical assay for red blood cells parasitized by Plasmodium falciparum," *Lab on a Chip,* vol. 12, pp. 1143-1150, 2012.

[13] W. J. Zhang, K. Kai, D. S. Choi, T. Iwamoto, Y. H. Nguyen, H. L. Wong*, et al.*, "Microfluidics separation reveals the stem-cell-like deformability of tumor-initiating cells," *Proceedings of the National Academy of Sciences of the United States of America,* vol. 109, pp. 18707-18712, Nov 13 2012.

[14] M. J. Rosenbluth, W. A. Lam, and D. A. Fletcher, "Analyzing cell mechanics in hematologic diseases with microfluidic biophysical flow cytometry," *Lab on a Chip,* vol. 8, pp. 1062-1070, 2008.

[15] K. D. Nyberg, M. B. Scott, S. L. Bruce, A. B. Gopinath, D. Bikos, T. G. Mason*, et al.*, "The physical origins of transit time measurements for rapid, single cell mechanotyping," *Lab on a Chip,* vol. 16, pp. 3330-3339, 2016.

CONTACT

*W. Guan, tel: +1-814-8675748; wzg111@psu.edu